

Gravonuclear Instabilities in Post-Horizontal-Branch Stars

Allen V. Sweigart¹
John C. Lattanzio²
James P. Gray²
and Christopher A. Tout³

¹Laboratory for Astronomy and Solar Physics, NASA/Goddard Space Flight Center, USA

²Department of Mathematics and Statistics, Monash University, Australia

³Institute of Astronomy, Madingley Road, Cambridge, UK

Abstract: We investigate the gravonuclear instabilities reported by Bono et al. (1997a,b) during the onset of helium-shell burning at the end of the horizontal-branch (HB) phase. These instabilities are characterized by relaxation oscillations within the helium shell which lead to loops in the evolutionary tracks. We find the occurrence of these instabilities depends critically on how the breathing pulses are suppressed near the end of the HB phase. If they are suppressed by omitting the gravitational energy term in the stellar structure equations, then the helium profile within the core at the end of the HB phase will contain a broad region of varying helium abundance. The helium-burning shell which forms in this region is too thick to be unstable, and gravonuclear instabilities do not occur. If, on the other hand, the breathing pulses are suppressed by prohibiting any increase in the central helium abundance, then the final helium profile can exhibit a large discontinuity at the edge of the helium-exhausted core. The helium shell which forms just exterior to this discontinuity is then much thinner and can be thermally unstable. Even in this case, however, the gravonuclear instabilities disappear as soon as the nuclear burning broadens the helium shell into its characteristic S-shape. We conclude that the gravonuclear instabilities found by Bono et al. are a consequence of the ad hoc procedure used to suppress the breathing pulses.

1 Introduction

A number of intriguing astrophysical problems are associated with the termination of central helium burning in horizontal-branch (HB) stars. One example concerns the so-called “breathing pulses” of the convective core. While numerical algorithms for treating semiconvection (e.g., Robertson & Faulkner 1972) work quite effectively during most of the HB phase, they invariably fail once the central helium abundance Y_c falls below $\simeq 0.1$. At that time the convective core suddenly grows so large that it engulfs most of the previous semiconvective zone, thereby bringing so much fresh helium into the center that Y_c increases.

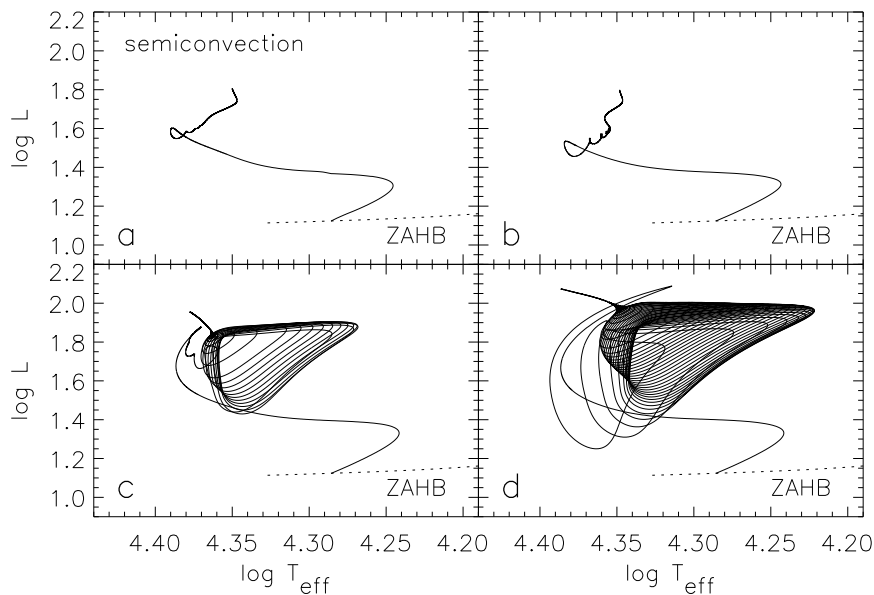


Figure 1: Evolutionary tracks for the HB and post-HB phases of a $0.48M_{\odot}$ star with $Z = 0.03$. Panel (a) gives a canonical semiconvection track computed with the $\epsilon_g = 0$ method for suppressing the breathing pulses during the core-helium-exhaustion phase. The tracks in panels (b), (c) and (d) were computed with the composition algorithm described in the text (see §2).

These breathing pulses are generally suppressed using one of the following methods:

- *Omission of gravitational energy term ϵ_g .* Dorman & Rood (1993) have shown that the breathing pulses can be suppressed by setting ϵ_g equal to 0 in the stellar structure equations during the core-helium-exhaustion phase. An example of a canonical HB and post-HB track computed with this approach is given in Figure 1a. Note that the evolution is quite smooth without any indication of an instability. The helium-burning luminosity L_{He} along this sequence, given in Figure 2a, shows only a characteristic dip at the end of the HB phase, as the helium burning shifts outward from the center to a shell. Most importantly, the composition profile within the core at the end of the HB phase contains a broad region of varying helium abundance Y corresponding to the former semiconvective zone (see Figure 3a).

- *Limit on growth of the convective core.* An alternative method for suppressing the breathing pulses, used by Bono et al. (1997a,b), is to limit the rate at which the convective core can grow in order to prevent Y_c from increasing. Inspection of Tables 1 – 5 of Castellani et al. (1991) shows that this ad hoc method leads to a greatly enlarged convective core that remains large until helium exhaustion. We infer therefore that the final helium profile should then contain a large discontinuity at the edge of the helium-exhausted core and thus should be markedly different from the profile produced by the first suppression method.

Bono et al. (1997a,b) recently argued that the onset of helium-shell burning in post-HB stars is dramatically different from the smooth evolution shown in Figure 1a, especially for metal-rich stars with low envelope masses. Their results indicate that the helium-burning shell undergoes a series of “gravonuclear instabilities” caused by relaxation oscillations similar to the helium-shell flashes that occur later on the asymptotic giant branch. These instabilities lead to pronounced “gravonuclear loops” (GNLs) along the evolutionary tracks, which could have interesting observational consequences. Figures 1d and 2d give examples of these GNLs and the associated helium-shell instabilities (see §2). We have undertaken extensive calculations to

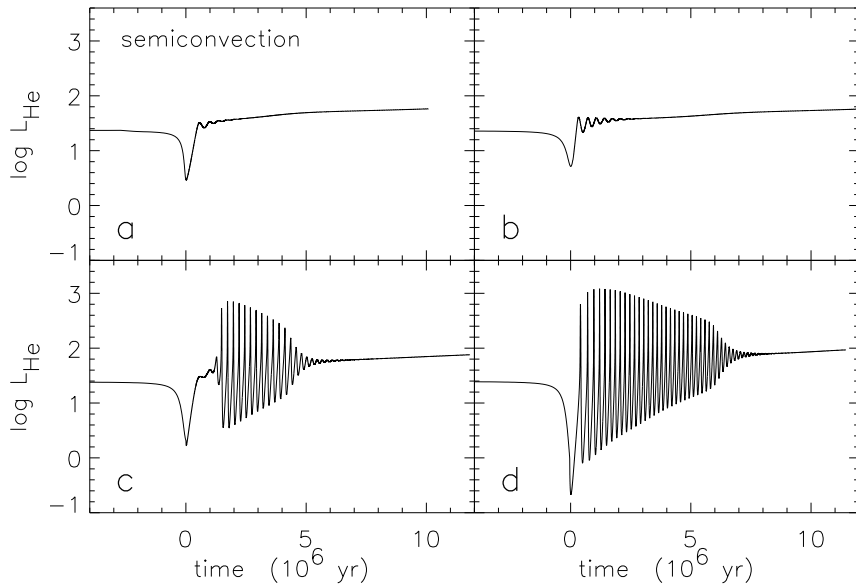


Figure 2: Time dependence of the helium-burning luminosity L_{He} during the post-HB evolution of the tracks in Figure 1. The zero point of the timescale corresponds to the minimum in L_{He} at the end of the HB phase. Each panel refers to the corresponding panel in Figure 1.

understand the cause of these gravonuclear instabilities. Our main conclusions are:

The occurrence of gravonuclear instabilities depends critically on the helium profile within the core at the end of the HB phase and hence on the method used to suppress the breathing pulses. Gravonuclear instabilities are only found when there is a large discontinuity in the helium abundance, which forces the helium burning to be confined to a narrow region at the edge of the core. Contrary to the Bono et al. results, we find that gravonuclear instabilities are not caused by a high envelope opacity nor do they depend on the envelope mass. Rather, they are a consequence of the method used by Bono et al. to suppress the breathing pulses.

2 Dependence of Instabilities on Core-Helium Profile

We first explored the dependence of the gravonuclear instabilities on the composition profile within the core at the end of the HB phase. To do this, we computed a number of HB and post-HB evolutionary sequences for a star with a mass $M = 0.48M_{\odot}$ and a heavy-element abundance $Z = 0.03$ for various assumptions about the final composition profile. These model parameters were chosen to optimize the likelihood of gravonuclear instabilities according to the Bono et al. results. A very small time step of only 400 yr was used in the post-HB models in order to resolve any instabilities, if present. Moreover, a thermal stability analysis was performed on each of the $\simeq 30,000$ post-HB models in each sequence to search for any unstable modes.

Our first sequence was a canonical semiconvection sequence computed with the $\epsilon_g = 0$ method for suppressing the breathing pulses. The results, given in Figures 1a and 2a, show no signs of any instability. In particular, the onset of helium-shell burning is marked by only minor (and damped) ringing in the helium-burning luminosity. The composition profile for this sequence, given in Figure 3a, contains a discontinuity in the helium abundance at $M_r = 0.237M_{\odot}$ corresponding to the outer edge of the semiconvective zone at its maximum extent during the HB phase. Interior to this discontinuity there is a broad region of varying helium

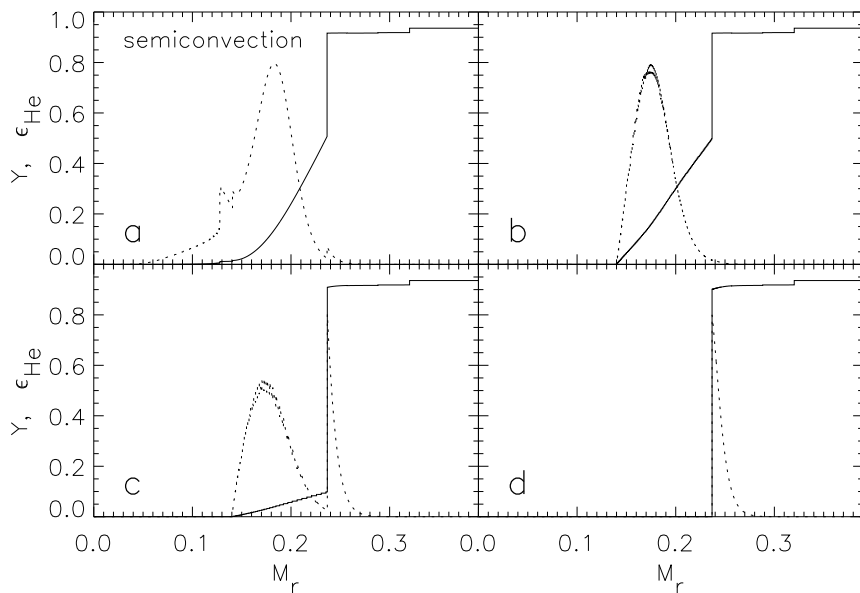


Figure 3: Helium profiles at central helium exhaustion for the sequences in Figures 1 and 2 (solid curves). The mass M_r is in solar units. The helium-burning rate ϵ_{He} (arbitrary units) is shown by dotted curves. Panels (a)–(d) correspond to the panels in Figures 1 and 2.

abundance which also is a remnant of the previous semiconvection and which we will refer to as the “helium tail”. Note that the helium burning in Figure 3a covers a wide range in mass.

We repeated these calculations using a “composition algorithm” to specify the size of the helium-depleted region instead of the canonical semiconvection algorithm. Essentially we required that the composition be completely mixed from the center out to a specified mass point in each model regardless of whether this region was fully convective. No mixing was permitted outside this point. By varying the size of this mixed region during the HB evolution we were able to generate different composition profiles having more or less steep helium tails at core-helium exhaustion. All these profiles had a helium discontinuity at $M_r = 0.237M_\odot$, as found with canonical semiconvection. This composition algorithm was turned off at the end of the HB, and post-HB evolution was then followed in the same manner as the canonical case.

Figures 1b, 2b and 3b present the results for a sequence computed with this algorithm. The final composition profile given in Figure 3b was chosen to mimic the composition profile for the semiconvection sequence given in Figure 3a. The resulting track morphology and helium-burning luminosity are virtually identical to those for the semiconvection sequence. Moreover, no thermally unstable modes were found. This indicates that the post-HB evolution is not sensitive to how the composition profile at the end of the HB phase is actually produced.

We then used our composition algorithm to compute sequences with shallower helium tails. No gravonuclear instabilities were found until the size of the helium tail was reduced to that shown in Figure 3c. The helium burning in Figure 3c initially covered a broad region within the helium tail, and the models were then stable. After $\simeq 10^6$ yr following core-helium exhaustion, however, this helium tail burned away, and the helium burning then shifted outward to a narrow region just outside the helium discontinuity. The helium burning immediately became unstable, giving rise to the flashes in Figure 2c and the GNLs in Figure 1c. The stability analysis of these models revealed the existence of thermally unstable modes.

We have also considered the limiting case of a helium discontinuity and no tail (Figure 3d).

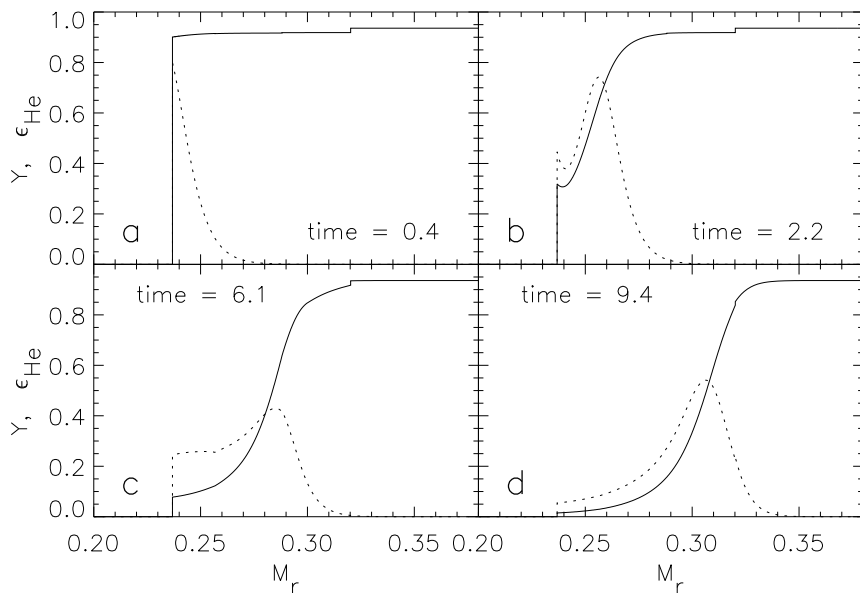


Figure 4: Helium profiles at various times during the post-HB evolution of the sequence in Figure 2d (solid curves). The helium-burning rate ϵ_{He} is shown in arbitrary units by the dotted curves. The times in each panel refer to the timescale in Figure 2d in units of 10^6 yr.

As shown in Figures 1d and 2d, such a profile leads to strong gravonuclear instabilities and to large GNLs. The composition profile in Figure 3d should be similar to the profile produced by the Bono et al. method for suppressing the breathing pulses. Note that this method forces the helium burning to be confined to a narrow region just outside the helium discontinuity.

The above results are not surprising. Schwarzschild & Härm (1965) showed that a nuclear burning shell must be thin to be unstable. Figures 1, 2 and 3 confirm that gravonuclear instabilities do not occur when the helium-burning region is broad. Only when the composition profile confines the burning to a narrow region, as in Figure 3d, do we find gravonuclear instabilities.

As further confirmation of this result, Figure 4 shows the helium profile at four times during the post-HB evolution of the sequence plotted in Figures 1d, 2d and 3d. Panel (a) is the same as Figure 3d and corresponds to the onset of gravonuclear instability. Panel (b) shows the helium profile during the period of strong gravonuclear instability, while panel (c) shows the helium profile for the last model in which we found thermally unstable modes. The helium-burning region in Figure 4 progressively broadens with time until by panel (d) the models are completely stable. We conclude therefore that the gravonuclear instabilities disappear as soon as the helium-burning region broadens into its characteristic S-shape profile.

3 Dependence of Instabilities on Envelope Mass and Z

We have also investigated whether the gravonuclear instabilities depend on the envelope mass and metallicity, as suggested by Bono et al. Figure 5 shows the time dependence of L_{He} during the post-HB evolution of four sequences with $M = 0.70M_{\odot}$ (and hence larger envelope mass). The composition profiles at the end of the HB phase for these sequences are virtually identical to those in the corresponding panels of Figure 3. Figure 5 shows the same overall behavior of L_{He} as Figure 2, except for the shorter timescale of the instabilities caused by the higher L_{He} of these higher mass sequences. It is clear therefore that the occurrence of gravonuclear instabilities does

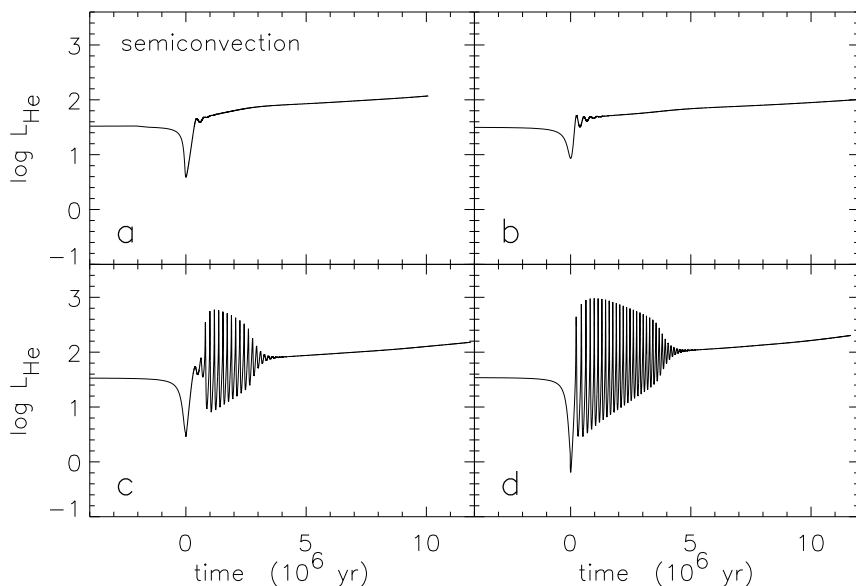


Figure 5: Same as Figure 2 except for a $0.70M_{\odot}$ star.

not depend on the envelope mass. The same conclusion applies to the metallicity. Calculations for a $M = 0.52M_{\odot}$, $Z = 0.002$ sequence, computed for the same helium profile as in Figure 3d, show extensive GNLs just as for our higher metallicity sequences.

4 Conclusions

Extensive calculations obtained with three independent stellar evolution codes have enabled us to consistently induce or remove GNLs according to the helium-composition profile at the end of core-helium burning. We have shown that GNLs are not favored by higher metallicities or lower masses, as postulated by Bono et al. (1997a,b). Rather, GNLs are produced by the narrowness of the helium-burning region when the helium-burning shell ignites immediately following core-helium exhaustion. This is most influenced by the way that the convective and semiconvective regions are calculated at the completion of core-helium burning and further illustrates our incomplete knowledge of this complicated phase. If we could observationally determine the existence, or otherwise, of GNLs, it would be a direct probe into the helium profile at helium exhaustion and hence provide information about the occurrence of core-breathing pulses.

References

- Bono, G., Caputo, F., Cassisi, S., Castellani, V. & Marconi, M. 1997a, ApJ, 479, 279
- Bono, G., Caputo, F., Cassisi, S., Castellani, V. & Marconi, M. 1997b, ApJ, 489, 822
- Castellani, V., Chieffi, A., & Pulone, L. 1991, ApJS, 76, 911
- Dorman, B., & Rood, R. T. 1993, ApJ, 409, 387
- Robertson, J. W., & Faulkner, D. J. 1972, ApJ, 171, 309
- Schwarzschild, M., & Härm, R. 1965, ApJ, 142, 855